

Structure and Photosynthetic Mimicking of Bis(2,6-bis(benzimidazol-2-yl)pyridine)manganese(II)

SHI, Wei^a(施伟) LI, Wei^{a,b}(李伟) SHEN, Ping-Ping^b(沈萍萍) XU, Ying-Kai^a(徐英凯)
WANG, Hong-Mei^a(王红梅) SHI, Mei^a(石梅) LIU, Yang^{*a}(刘扬)

^aState Key Laboratory for Structural Chemistry of Unstable and Stable Species, Center of Molecular Science, Institute of Chemistry, Chinese Academic of Sciences, Beijing 100080, China

^bState Key Laboratory of Pharmaceutical Biotechnology, Department of Biochemistry, Nanjing University, Nanjing, Jiangsu 210008, China

Mn(bzimpy)₂(1) [bzimpy = 2,6-bis(benzimidazol-2-yl)pyridine], a mononuclear manganese(II) complex, was synthesized by the reaction of Mn(OOCMe)₂ with bzimpy in absolute ethanol. The complex was structurally characterized by elemental analysis, cyclic voltammetry, and X-ray crystallography. In the complex, the manganese-nitrogen distances were different, and the geometry and the metal ion environment showed the distortion. The cyclic voltammetric measurements have been performed to assess its redox characteristics. The presence of oxidation wave at +0.62 V and +0.81 V vs. SCE or +0.8 V and +1.0 V vs. NHE suggested that this complex could catalyze the oxidation of water, therefore, simulate the water-oxidizing complex (WOC) of photosystem II (PS II). The measurements of photoreduction of 2,6-dichlorophenolindophenol (DCPIP), and oxygen evolution in the manganese-depleted and the complex 1-reconstituted PS II preparations just support our conjecture.

Keywords 2,6-bis(benzimidazol-2-yl)pyridine (bzimpy), crystal structure, photosynthetic mimicking

Introduction

Manganese ions play an important role in the light-induced oxidation of water to molecular oxygen in photosystem II (PS II) of green plants.¹⁻³ In recent years, manganese complexes of polypyridine ligands, such as bipyridine, 1,10-phenanthroline and 2,2':6',2''-terpyridine, have had considerable attention as the complexes formed are useful models for manganese-containing bimoleculars.⁴⁻⁶ Therefore, synthesis and characterization of manganese in its various oxidation states, with various ligand types and nuclearities, have contributed substantially to our understanding of the role and mechanism of manganese complexes in photosynthesis.

The prevalent notion is that the water-oxidizing complex (WOC) of PS II is a tetranuclear manganese cluster. The current model for the assembly of the manganese clus-

ter of WOC during photoactivation indicates that the first two manganese are integrated sequentially followed by the relatively slow attachment of the two additional manganese atoms.⁷⁻⁹ From this point of view, the mononuclear manganese complex may also be able to bring about the sequential addition of four individual manganese atoms and reconstitute WOC.

Ligand of the title complex comprises a donor group of relevance to the coordination of metal centers in many biological systems, namely imidazole (histidine). Thus, here we report the synthesis, crystal structure and electrochemical characterization of complex 1, Mn(bzimpy)₂[bzimpy = 2,6-bis(benzimidazol-2-yl)pyridine], and its photosynthetic mimicking.

Experimental

Materials and methods

Ethanol and dimethylsulfoxide were purified by distillation. Tetrabutylammonium hexafluorophosphate was obtained from Wako Chemical Co. and manganese acetate was from Aldrich. The bzimpy was prepared from 2,6-pyridinedicarboxylic acids as the reported method.¹⁰ PS II membrane was prepared from spinach as described by Kuwabara and Murata.¹¹ Extraction of Mn was performed as the method reported previously.¹²

Preparation of the title complex 1

The complex was prepared by addition of Mn(OAc)₂ (0.09 g, 0.26 mmol) in ethanol (10 mL) to a stirred solution of 2,6-bis(benzimidazol-2-yl)pyridine (0.16 g, 0.538 mmol) in absolute ethanol (30 mL). The resulting solution was stirred at 50 °C for 30 min and yellow precipi-

E-mail: yliu@iccas.ac.cn

Received July 19, 2002; revised November 28, 2002; accepted February 20, 2003.

Project supported by the Major State Basic Research Development Program (No. G1998010100) and the National Natural Science Foundation of China (Nos. 39890390 and 39870208).

tate was collected by filtration, washed with ethanol, and dried *in vacuo*. The precipitate was dissolved in dimethylsulfoxide and the solution was filtered. The filtrate was layered with EtOH to produce yellow crystal in one week (yield 0.09 g, 52%). M. p. 428–431 °C; FT-IR (KBr) ν : 3054, 1601, 1574, 1502, 1450 cm^{-1} . Anal. calcd for $\text{C}_{38}\text{H}_{24}\text{MnN}_{10}$: C 67.4, H 3.6, N 20.7; found C 67.5, H 3.8, N 20.5.

X-Ray crystallographic data collection and refinement of structure

Single crystal of the complex **1** was selected and mounted on the goniometer of Rigaku R-AXIS RAPID imaging plate diffractometer. Diffraction data were collected at 293 K with graphite monochromated Mo $K\alpha$ radiation ($\lambda = 0.07107$ nm) operating at 50 kV and 3 mA. The detector swing angle was 5.00°. Readout was performed in the 0.100 mm pixel mode. Absorption corrections were applied by correlation of symmetry-equivalent reflections using the ABSOR program. Data reduction was performed by SHELX97 (Sheldrick, 1997). The structure was solved by direct method and difference Fourier map using SHELXS97 (Sheldrick, 1997) and refined on F^2 by full-matrix least-squares techniques using SHELXL97 (Sheldrick, 1997). The data collection and structure solution parameters and conditions are listed in Table 1. Selected bond lengths and angles are listed in Tables 2 and 3.

Table 1 Crystallographic data of complex $\text{Mn}(\text{bzimpy})_2$

Empirical formula	$\text{C}_{38}\text{H}_{24}\text{N}_{10}\text{Mn}$
Formula weight	675.61
Crystal size (mm)	$0.35 \times 0.14 \times 0.11$
Crystal color	Yellow
Crystal system	Monoclinic
Space group	Pn
a (nm)	1.02422(18)
b (nm)	1.01588(12)
c (nm)	1.6012(2)
β (°)	90.72(3)
V (nm^3)	1.6659(4)
Z	2
T (K)	293(2)
D_{calc} (Mg/m^3)	1.347
Absorption coefficient (mm^{-1})	0.440
$F(000)$	694
θ Range for data collection	2.00–27.48
Reflections collected/unique	6041/6037 [$R_{\text{int}} = 0.1330$]
Completeness to $\theta = 27.48$	94.9%
Data/restraints/parameters	6037/2/447
Goodness of fit on F^2	0.948
Final R indices [$I > 2\sigma(I)$]	$R = 0.0717$; $wR = 0.1830$
Largest difference peak and hole (e/nm^3)	267 and -288

Table 2 Selected bond lengths (nm) for $\text{Mn}(\text{bzimpy})_2$

Atom	Bond length	Atom	Bond length
Mn(1)—N(3)	0.2220(6)	Mn(1)—N(5)	0.2229(7)
Mn(1)—N(10)	0.2230(6)	Mn(1)—N(8)	0.2253(6)
Mn(1)—N(1)	0.2239(6)	Mn(1)—N(6)	0.2265(6)
N(1)—C(6)	0.1354(9)	N(1)—C(7)	0.1364(9)
N(2)—C(7)	0.1348(9)	N(2)—C(1)	0.1396(10)
N(3)—C(12)	0.1325(10)	N(3)—C(8)	0.1365(10)
N(6)—C(26)	0.1353(9)	N(6)—C(25)	0.1390(10)
N(7)—C(26)	0.1356(10)	N(7)—C(20)	0.1391(10)
N(8)—C(27)	0.1327(10)	N(8)—C(31)	0.1354(10)
C(1)—C(2)	0.1368(11)	C(4)—C(5)	0.1360(13)
C(1)—C(6)	0.1401(10)	C(2)—C(3)	0.1340(12)
C(3)—C(4)	0.1428(13)	C(5)—C(6)	0.1438(10)
C(7)—C(8)	0.1445(10)	C(8)—C(9)	0.1440(11)
C(9)—C(10)	0.1320(15)	C(10)—C(11)	0.1377(14)
C(11)—C(12)	0.1396(11)	C(30)—C(31)	0.1391(11)
C(20)—C(21)	0.1369(12)	C(20)—C(25)	0.1426(11)
C(21)—C(22)	0.1405(13)	C(22)—C(23)	0.1403(13)
C(23)—C(24)	0.1394(13)	C(24)—C(25)	0.1360(11)
C(26)—C(27)	0.1491(11)	C(27)—C(28)	0.1357(11)
C(28)—C(29)	0.1349(16)	C(29)—C(30)	0.1397(15)

Table 3 Selected bond angles ($^{\circ}$) for $\text{Mn}(\text{bzimpy})_2$

Atom	Angle	Atom	Angle
N(1)-Mn(1)-N(5)	145.2(2)	N(5)-Mn(1)-N(10)	105.0(2)
N(1)-Mn(1)-N(3)	73.0(2)	N(1)-Mn(1)-N(10)	84.8(2)
N(3)-Mn(1)-N(5)	72.2(2)	N(5)-Mn(1)-N(8)	107.8(2)
N(3)-Mn(1)-N(8)	179.1(3)	N(1)-Mn(1)-N(8)	107.0(2)
N(6)-Mn(1)-N(10)	145.0(2)	N(3)-Mn(1)-N(6)	107.8(2)
N(6)-Mn(1)-N(8)	71.3(2)	N(8)-Mn(1)-N(10)	73.7(2)
N(5)-Mn(1)-N(6)	85.9(2)	N(6)-Mn(1)-N(1)	105.2(2)
N(3)-Mn(1)-N(10)	107.2(2)		

Measurements

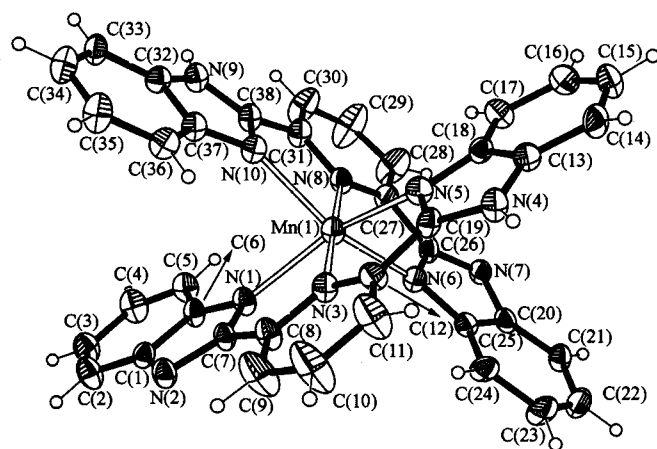
The FT-IR spectra were measured as KBr pellets on a Perkin-Elmer System 2000 spectrometer. Elemental analyses were carried out on a Carlo-Erbla 1160 elemental analyzer. Electrochemical measurements were recorded using a CHI 705A Electrochemical Analyzer. The cyclic voltammetry was conducted in a standard three-electrode cell. A glassy carbon electrode (2 mm diameter) was used as the working electrode; a platinum wire as the counter electrode and a saturated calomel electrode (SCE) as the reference electrode. The scan rate was $30 \text{ mV} \cdot \text{s}^{-1}$. Anhydrous dimethyl sulfoxide was used as the solvent. The supporting electrolyte was tetrabutylammonium hexafluorophosphate (0.1 mol/L). The rate of oxygen evolution was monitored at $20 \text{ }^{\circ}\text{C}$ with a Clark-type electrode.¹³ The assay medium contained the preparations of PS II membrane at a concentration of $10 \mu\text{g Chl/mL}$, $25 \text{ mmol/L Mes-NaOH}$ ($\text{pH} = 6.5$), 5 mmol/L CaCl_2 , 10 mmol/L NaCl , $300 \text{ mmol/L sucrose}$ and $200 \mu\text{mol/L phenyl-}p\text{-benzoquinone}$, $300 \mu\text{mol/L potassium ferricyanide}$ as electron acceptor. The photoreduction of 2,6-dichlorophenolindophenol (DCPIP) was measured at $20 \text{ }^{\circ}\text{C}$ using a spectrophotometer (Shimadzu UV-160 lpc UV-visible). The reaction medium consisted of the preparations of PS II membrane at a concentration of $10 \mu\text{g Chl/mL}$, $20 \text{ mmol/L Tris-HCl}$ ($\text{pH} 7.8$), 10 mmol/L NaCl , 2 mmol/L MgCl_2 and $50 \mu\text{mol/L DCPIP}$.

Results and discussion

Crystal structure

The structure of complex 1 and the atom numbering scheme are shown in Fig. 1. Selected bond lengths and bond angles are listed in Tables 2 and 3, respectively.

The complex shows that the expected structure with two meridionally coordinated tridentate bzimpy ligands gives a distorted octahedral coordination of the manganese as observed for $[\text{Mn}(\text{terpy})_2]^{2+}$ in $\text{Mn}(\text{terpy})_2(\text{I}_3)_2$.¹⁴ Two $\text{Mn}-\text{N}_{\text{py}}$ bonds in complex 1 are almost co-linear [$\text{N}_3\text{-Mn}_1\text{-N}_8$, $179.1(3)^{\circ}$] as found in $[\text{Mn}(\text{terpy})_2]^{2+}$ where the equivalent angle is $177.1(5)^{\circ}$, and in $[\text{Fe}(\text{bzimpy})_2]^{2+}$ where the equivalent angle is $176.8(4)^{\circ}$.¹⁵ The average N-Mn-N chelate angle is 72.5° compared with 79.5° for $[\text{Fe}(\text{bzimpy})_2]^{2+}$ and 80.6° for $[\text{Mn}(\text{terpy})_2]^{2+}$ complex.

**Fig. 1** Structure of the complex $\text{Mn}(\text{bzimpy})_2$.

The average $\text{Mn}-\text{N}$ bond distance (0.2239 nm) in $\text{Mn}(\text{bzimpy})_2$ is identical to the value for $[\text{Mn}(\text{terpy})_2]^{2+}$ (0.2232 nm) within experimental error. The $\text{Mn}-\text{N}$ bond length in $[\text{Mn}(\text{terpy})_2]^{2+}$ shows considerable asymmetry, *i.e.*, the $\text{Mn}-\text{N}_{\text{central}}$ distances are nearly $0.006(2) \text{ nm}$ shorter than the $\text{Mn}-\text{N}_{\text{terminal}}$ distances. Similarly, the $\text{Fe}-\text{N}_{\text{py}}$ bond distances are also shorter than the other $\text{Fe}-\text{N}$ distances in $[\text{Fe}(\text{bzimpy})_2]^{2+}$ by $0.006(1) \text{ nm}$. In $\text{Mn}(\text{bzimpy})_2$, there is a distortion of the coordination sphere in which the average $\text{Mn}-\text{N}_{\text{py}}$ distance, $0.2237(1) \text{ nm}$, is slight shorter than the average of other $\text{Mn}-\text{N}$ distance, $0.2241(4) \text{ nm}$. The distortion can always be observed in terpyridyl complexes of the first-row transition metal complexes,¹⁶⁻¹⁸ which was thought to be due to better overlap of the metal t_{2g} orbitals with the π^* orbitals of the central pyridyl group in comparison with the distal pyridyl groups.¹⁹ In addition, the MnN_6 coordination shows appreciable angular distortions. The $\text{N}_1\text{-Mn}_1\text{-N}_3$, $\text{N}_5\text{-Mn}_1\text{-N}_3$, $\text{N}_6\text{-Mn}_1\text{-N}_8$, and $\text{N}_{10}\text{-Mn}_1\text{-N}_8$ angles deviate from 90° by 17° , 17.8° , 18.7° and 16.3° , respectively.

The crystal packing shows that the $\text{Mn}(\text{bzimpy})_2$ molecules are packed in planes. The complex 1 features a

layer crystal structure, which may be conveniently described with reference to the hydrogen bonds scheme shown in Fig. 2. Each ligand formed two hydrogen bonds: (A) $N-H \cdots N$ (B), 0.2778 nm, and (A) $N \cdots H-N$ (C), 0.2741 nm, where A, B, C represent different molecules, and N is uncoordinated nitrogens of the benzimidazole rings. The lattice of parameters complex **1** can be contrasted with that of a similar complex, $[Mn(bzimpy)_2] \cdot EtOOCMe \cdot H_2O$, in which the crystal space group is *Cc* [$a = 1.3644(1)$ nm, $b = 1.5309(2)$ nm, $c = 1.8558(3)$ nm, $\beta = 110.28(1)^\circ$].²⁰ Although both of them are built from the same ligand, their packing modes are different, which may contribute to the subsistence of the solvent molecules inside the crystal of $[Mn(bzimpy)_2] \cdot EtOOCMe \cdot H_2O$.

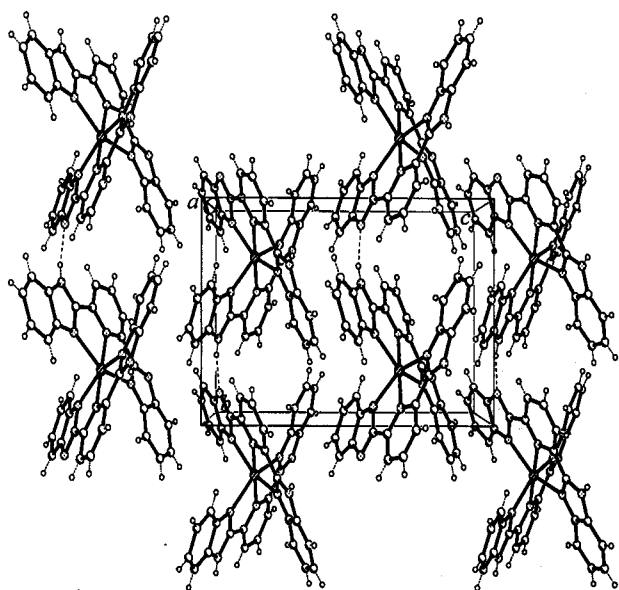


Fig. 2 Representation of the crystal packing in $Mn(bzimpy)_2$. The dotted lines represent the H-bonding interactions $N-H \cdots N$.

Photosynthetic mimicking

Cyclic voltammetry

A necessary criterion for the design of model systems for the water oxidation reaction in PS II is that the model system must have redox potential more (or at least as) positive than (as) the minimum of +0.6 V vs. NHE required to oxidize water to oxygen at pH 7 in the biomembrane.²¹ So the redox potential of complex **1** was examined by cyclic voltammetry. The result shows two oxidation peaks in the positive potential region (Fig. 3). The literature data abound with a diversity of redox potentials for $Mn(II)-Mn(III)$ and $Mn(III)-Mn(IV)$ couples.²²⁻²⁵ In light of literature values, the waves of +0.62 V and +0.81 V vs. SCE for the complex **1** can be assigned to two successive oxidations of $Mn(II)$ to $Mn(III)$ and $Mn(IV)$.

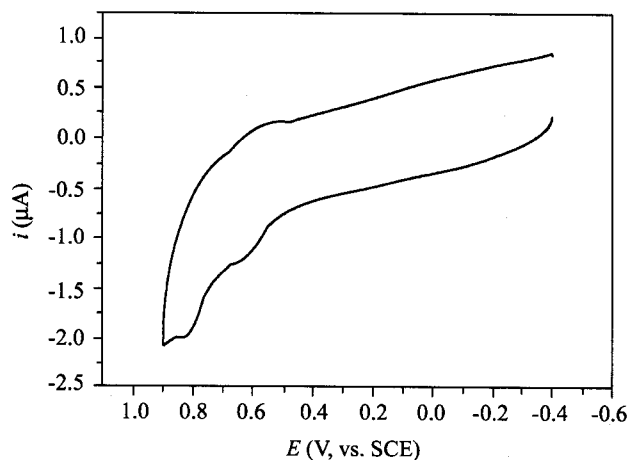


Fig. 3 Oxidative voltammogram of the complex $Mn(bzimpy)_2$ in dimethyl sulfoxide.

Additionally, the complex **1** undergoes two reduction processes in negative potential region of -1.2 V to -1.8 V vs. SCE (Fig. 4), which may be assigned to the reduction process of the ligand itself. Assignment of the ligand-centered reduction peaks was based on a recent study of manganese, cobalt and iron complexes with a variety of ligands.²⁶

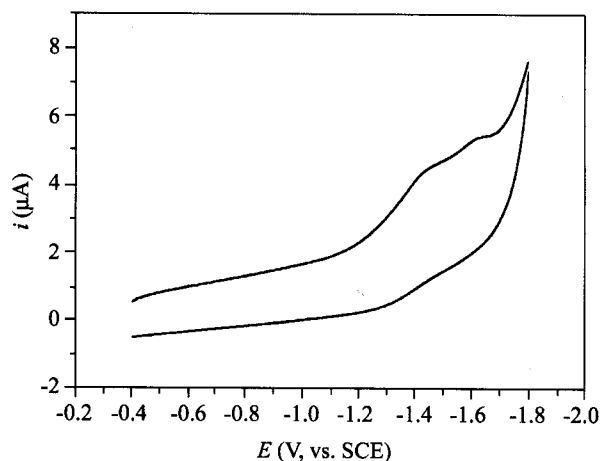


Fig. 4 Reductive voltammogram of the complex $Mn(bzimpy)_2$ in dimethyl sulfoxide.

Because the complex **1** with its oxidation potential at +0.62 and 0.81 V vs. SCE or *ca.* +0.8 and 1.0 V vs. NHE is obviously more positive than +0.6 V vs. NHE that required for the water oxidation at pH 7 in the photosystem,²¹ we further performed the measurements of photoreduction of DCPIP and oxygen evolution in the manganese-depleted PS II and the complex **1** reconstituted PS II preparations.

Photoreduction of DCPIP and oxygen evolution measurements

Reconstruction of electron transport capacity was

demonstrated by the experiments using DCPIP as the final electron acceptor (Fig. 5). The initial rate of DCPIP photoreduction in Mn-depleted preparations was severely reduced in comparison with native PS II preparations (control). Photoreduction was greatly restored in the presence of either MnCl_2 or the complex **1**. The oxygen-evolving activities of the PS II membrane and the other reconstructed Mn-depleted preparations are listed in Table 4. The oxygen activity was almost completely inhibited in the Mn-depleted samples, and can be partially recovered when MnCl_2 was added. Moreover, the addition of complex **1** yielded an even greater initial rate of oxygen evolution than that in the reconstructed MnCl_2 , as shown in Table 4.

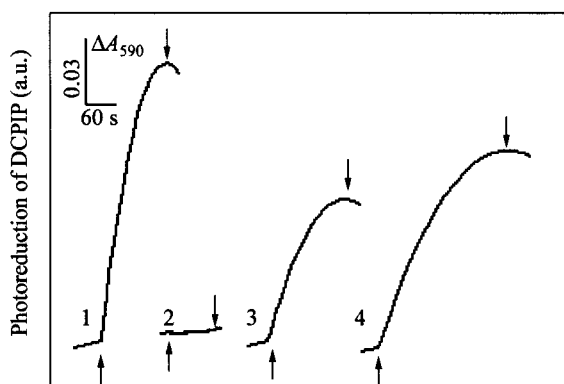


Fig. 5 Photoreduction of DCPIP measured at 590 nm in DT20 preparations. Trace 1, control; trace 2, Mn depleted; trace 3, reconstituted with 1 $\mu\text{mol/L}$ MnCl_2 ; trace 4, reconstituted with 1 $\mu\text{mol/L}$ complex **1**.

Table 4 Reactivation of oxygen evolution in Mn-depleted preparations^a

	Initial rate of oxygen evolution ($\mu\text{mol O}_2/\text{mg Chl h}$)
Native preparations	268
Mn-depleted	0
Mn-depleted + MnCl_2	37
Mn-depleted + Mn complex	88

^a MnCl_2 and Mn complex were added at a concentration of 2 $\mu\text{mol/L}$.

Observations of electron transport and oxygen evolution obviously show that Mn complex can reconstruct the WOC in Mn-depleted PS II preparations. It is noteworthy that complex **1**, as an electron donor, is more efficient than Mn-Niten complex and Mn-Salhx complex.²⁷ It is likely that the complex **1** contains pyridine and benzimidazole rings, which facilitate interaction with the exposed donor side of PSII. Therefore, the complex **1** gains more accessibility to the Mn oxidation sites in the protein matrix, which brings about the restore of DCPIP photoreduction and higher rates of oxygen evolution after the reconstruction.

Above all, our results clearly demonstrate that mononuclear complex **1** is able to reconstitute the WOC of

PS II in plant photosynthesis with a significantly greater efficiency.

References

- 1 Debus, R. J. *Biochim. Biophys. Acta* **1992**, *1102*, 269.
- 2 Yachandra, V. K.; Sauer, K.; Klein, M. P. *Chem. Rev.* **1996**, *96*, 2927.
- 3 Limburg, J.; Vrettos, J. S.; Liable-Sands, L. M.; Rheingold, A. L.; Crabtree, R. H.; Brudvig, G. W. *Science* **1999**, *283*, 1524.
- 4 (a) Wieghardt, K. *Angew. Chem.* **1989**, *101*, 1179.
(b) Wieghardt, K. *Angew. Chem., Int. Ed. Engl.* **1989**, *28*, 1153.
- 5 Collomb, M. N.; Deronzier, A.; Richardot, A.; Pecaut, J. *New J. Chem.* **1999**, *23*, 351.
- 6 Limburg, J.; Vrettos, J. S.; Chen, H.; Paula, J. C.; Crabtree, R. H.; Brudvig, G. W. *J. Am. Chem. Soc.* **2001**, *123*, 423.
- 7 Tamura, N.; Cheniae, G. M. *Biochim. Biophys. Acta* **1987**, *890*, 179.
- 8 Blubaugh, D.; Cheniae, G. M. *Research in Photosynthesis*, Ed.: Murata, N., Kluwer Academic, Dordrecht, **1992**, pp. 361–364.
- 9 Miller, A. F.; Brudvig, G. W. *Biochemistry* **1990**, *29*, 1385.
- 10 Addison, A. W.; Burke, P. J. *J. Heterocyclic. Chem.* **1981**, *18*, 803.
- 11 Kuwabara, T.; Murata, N. *Plant Cell Physiol* **1982**, *23*, 533.
- 12 Allakhverdiev, S. I.; Karacan, M. S.; Somer, G.; Karacan, N.; Khan, E. M.; Rane, S. Y.; Padhve, S.; Klumov, V. V. *Renger. Biochemistry* **1994**, *33*, 12210.
- 13 Carpentier, R.; LaRue, B.; Leblanc, M. R. *Arch. Biochem. Biophys.* **1984**, *228*, 534.
- 14 Bhula, R.; Weatherburn, D. C. *Aust. J. Chem.* **1991**, *44*, 303.
- 15 Piguet, C.; Bocquet, B.; Muller, E.; Williams, A. F. *Helv. Chim. Acta* **1988**, *72*, 323.
- 16 (a) Figgis, B. N.; Kucharski, E. S.; White, A. H. *Aust. J. Chem.* **1983**, *36*, 1527.
(b) Figgis, B. N.; Kucharski, E. S.; White, A. H. *Aust. J. Chem.* **1983**, *36*, 1537.
- 17 Bsker, A. T.; Goodwin, H. A. *Aust. J. Chem.* **1985**, *38*, 207.
- 18 (a) Arriortua, M. I.; Rojo, T.; Amigo, J. M.; Germaine, G.; Declercq, J. P. *Bull. Soc. Chim. Belg.* **1982**, *91*, 337.
(b) Arriortua, M. I.; Rojo, T.; Amigo, J. M.; Germaine, G.; Declercq, J. P. *Acta Crystallographica. Sect. B* **1982**, *38*, 1323.
- 19 Figgis, P. E.; Busch, D. H. *J. Phys. Chem.* **1961**, *65*, 2236.
- 20 Rajan, R.; Rajaram, R.; Nair, B. U.; Ramasami, T.; Mandal, S. K. *J. Chem. Soc., Dalton Trans.* **1996**, 2019.

- 21 Matsushita, T.; Spencer, L.; Sawyer, D. T. *Inorg. Chem.* **1988**, *27*, 1167.
- 22 Neves, A.; Erthal, S. M. D.; Vencato, I.; Ceccato, A. S.; Mascarenhas, Y. P.; Nascimento, O. R.; Hörner, M.; Batista, A. A. *Inorg. Chem.* **1992**, *31*, 4749.
- 23 Ramesh, K.; Bhuniya, D.; Mukherjee, R. *J. Chem. Soc., Dalton Trans.* **1991**, 2917.
- 24 Luaces, L.; Bermejo, M. R.; Garcia-Vasquez, J. A.; Romero, J.; Sousa, A.; Watkinson, M.; Mugnier, Y.; McAuliffe, C. A.; Pritchard, R. C.; Helliwell, M. *Polyhedron* **1996**, *15*, 1375.
- 25 Bermejo, M. R.; Castineiras, A.; Garcia-Monteagudo, J. C.; Rey, M.; Sousa, A.; Watkinson, M.; McAuliffe, C. A.; Pritchard, R. C.; Beddoes, R. L. *J. Chem. Soc., Dalton Trans.* **1996**, 2935.
- 26 Richert, S. A.; Tsang, P. K. S.; Sawyer, D. T. *Inorg. Chem.* **1988**, *27*, 1814.
- 27 Allakhverdiev, S. I.; Ozdemir, U.; Harnois, J.; Karacan, N.; Hotchandani, S.; Klimov, V. V.; Murata, N.; Carpentier, R. *Photochemistry and Photobiology* **1999**, *70*, 57.

(E0207192 ZHAO, X. J.)